Performance of various correlation measures in quantum phase transitions using the quantum renormalization-group method

Yao Yao, Hong-Wei Li, Chun-Mei Zhang, Zhen-Qiang Yin,* Wei Chen, Guang-Can Guo, and Zheng-Fu Han†
Key Laboratory of Quantum Information, University of Science and Technology of China, Hefei 230026, China
(Received 11 June 2012; revised manuscript received 24 July 2012; published 3 October 2012)

We have investigated the quantum phase transition employing the quantum renormalization-group method while, in most of the previous literature, entanglement (concurrence) has been barely demonstrated. However, it is now well known that entanglement is not the only signature of quantum correlations and a variety of computable measures have been developed to characterize quantum correlations in the composite systems. As an illustration, two cases are elaborated: a one-dimensional anisotropic (i) XXZ model and (ii) an XY model, with various measures of quantum correlations, including quantum discord, geometric discord, measurement-induced disturbance, measurement-induced nonlocality, and violation of Bell inequalities [e.g., Clauser-Horne-Shimony-Holt (CHSH) inequality]. We have proved that all of these correlation measures can effectively detect the quantum critical points associated with quantum phase transitions after several iterations of the renormalization in both cases. Nonetheless, it is shown that some of their dynamical behaviors are not totally similar with entanglement and, even when concurrence vanishes, there still exists some kind of quantum correlation which is not captured by entanglement. Intriguingly, CHSH inequality can never be violated in the whole iteration procedure, which indicates that block-block entanglement cannot revealed by the CHSH inequality. Moreover, the nonanalytic and scaling behaviors of Bell violation have also been discussed in detail. As a by-product, we verify that measurement-induced disturbance is exactly equal to the quantum discord measured by σ_z for general X-structured states.

DOI: 10.1103/PhysRevA.86.042102 PACS number(s): 03.65.Ud, 03.67.Mn

I. INTRODUCTION

The origin of quantum correlation research or, more precisely, quantum entanglement can date back to a paper [1] in 1935, and nowadays there is no doubt that quantum entanglement is one of the most significant concepts in quantum information processing [2]. It has already been recognized as the fundamental feature of quantum mechanics and utilized as a crucial resource for communication and computation. However, entanglement should not be viewed as a unique measure of quantum correlations since there exist other types of nonclassical correlations which are not captured by entanglement. Recently, many authors have proposed a variety of computable measures to characterize quantum correlations in the composite states: quantum discord (QD) [3,4], geometric discord (GD) [5,6], measurement-induced disturbance (MID) [7], measurement-induced nonlocality (MIN) [8], ameliorated MID [9], and so on. Within such a quantum-classical framework, a great deal of concern has been raised by quantum discord and discord-like correlation measures in the past few years (for review, see Ref. [10] and references therein).

In particular, as an important application in quantum phase transition (QPT) [11], entanglement can be exploited to determine the critical points (CP) for spin chains at zero temperature [12–16]. Meanwhile, since quantum discord (and other discord-like measures) is introduced as an information-theoretical tool to qualify and quantify quantum correlations, it is natural for us to clarify the role played by quantum discord in QPT. Several studies concerning such a relationship have already appeared in Ref. [17–19]. These recent observations demonstrate that the CP information provided by QD is just in agreement with that of entanglement, and even at finite temperature QD still works fine [19].

Instead of resorting to two-point spin-spin correlation functions, which is usually done in most of the previous literature, the quantum renormalization-group (QRG) method [20,21] is introduced to investigate the quantum information properties of critical systems. Invoking such a method, surveys regarding Ising and Heisenberg models have been carried out in several works [22–27] and it has been shown that implementation of the QRG method is valuable in detecting the nonanalytic behavior of entanglement (concurrence) and the scaling behavior in the vicinity of CPs. Nevertheless, as mentioned above, entanglement is not sufficient to account for all the correlation contained in quantum systems, so this motivates us to apply other correlation witnesses to study their dynamic behaviors combining with QRG method. To serve as a further comparison, the violation of Bell inequalities [28,29] is also taken into consideration.

The outline of this paper is as follows. In Sec. II and Sec. III, we investigate a one-dimensional anisotropic XXZ model and XY model respectively, using several kinds of correlation indicators under the method of QRG. In Sec. IV, we discuss the scaling behavior of these quantifiers when close to CPs. Section V is devoted to the discussion and conclusion. Finally, some technical points are clarified in the Appendix.

II. CORRELATION ANALYSIS IN THE ANISOTROPIC XXZ MODEL

First, we recall the QRG method and its application in the one-dimensional anisotropic XXZ model. In fact,

*yinzheqi@mail.ustc.edu.cn
†zfhan@ustc.edu.cn

renormalization group refers to a mathematical tool that allows systematic investigation of the changes of a physical system as viewed at different distance scales. The key point to QRG scheme lies in reducing the effective degrees of freedom of the system through a recursive procedure until a mathematically tractable situation is reached. Following Kadanoff's approach (the "block-spin" renormalization group), the (one-dimensional) lattice is split into blocks. The Hamiltonian of each block is diagonalized exactly to obtain the low-lying eigenstates (project operator) to construct the basis for renormalized Hilbert space. Finally, the full Hamiltonian is projected onto the renormalized space to achieve an effective Hamiltonian H^{eff}. Here we can summarize the QRG method as the following steps:

(1) Decomposing the Hamiltonian into the intrablock and interblock parts: $H = H^B + H^{BB}$, where H^B is the block Hamiltonian, and the interblock interaction is denoted as H^{BB}.

(2) Diagonalization of H^B: this procedure is aiming to obtain the low-lying eigenstates and build the projection operator P_0 onto the the low-energy subspace.

(3) Renormalization of H^B and H^{BB}: by virtue of perturbative expansion (see Ref. [30]), the effective (renormalized) Hamiltonian up to the first-order correction is $H^{\text{eff}} = H_0^{\text{eff}} + H_1^{\text{eff}}$, where $H_0^{\text{eff}} = P_0 H^B P_0$ and $H_1^{\text{eff}} = P_0 H^{BB} P_0$.

(4) Iteration: repeat (1) $\Rightarrow$ (3) to arrive at the final manageable situation. For more details, we refer the readers to Refs. [30–32].

Kargarian *et al.* introduced the notion of "renormalization of concurrence" [22], and they found that this notion truly captures the nonanalytic behavior of the derivative of entanglement (concurrence) close to the critical point. As a warmup, we, first, review the renormalization of entanglement in the one-dimensional anisotropic XXZ model [23]. The Hamiltonian of spin 1/2 XXZ model on a periodic chain of N sites is

$$H(J,\Delta) = \frac{J}{4}\sum_i^N \left(\sigma_i^x\sigma_{i+1}^x + \sigma_i^y\sigma_{i+1}^y + \Delta\sigma_i^z\sigma_{i+1}^z\right), \quad (1)$$

where J is exchange constant, Δ is the anisotropy parameter, and $J,\Delta > 0$. $\sigma_i^\alpha (\alpha = x,y,z)$ are standard Pauli matrices at site i. This model is known to be exactly solvable by Bethe Ansatz and critical (gapless) while $0 \leqslant \Delta \leqslant 1$. The Ising regime is $\Delta > 1$ and a maximum of concurrence can be reached between two nearest-neighbouring spins at the transition point $\Delta = 1$ [33,34].

To construct a renormalized form for the Hamiltonian (1), we shall choose a decomposition of three-site blocks. Note that this is requisite in the sense that it is a guarantee of self-similarity after each iterative step. Reference [23] gives the degenerate ground states of the block Hamiltonian as follows

$$|\phi_0\rangle = \frac{1}{\sqrt{2+q^2}}(|\uparrow\uparrow\downarrow\rangle + q|\uparrow\downarrow\uparrow\rangle + |\downarrow\uparrow\uparrow\rangle), \quad (2)$$

$$|\phi_0'\rangle = \frac{1}{\sqrt{2+q^2}}(|\uparrow\downarrow\downarrow\rangle + q|\downarrow\uparrow\downarrow\rangle + |\downarrow\downarrow\uparrow\rangle), \quad (3)$$

where $|\uparrow\rangle, |\downarrow\rangle$ are the eigenstates of σ_z and

$$q = -\tfrac{1}{2}(\Delta + \sqrt{\Delta^2+8}). \quad (4)$$

The effective Hamiltonian of the renormalized chain then can be cast into the form

$$H^{\text{eff}} = \frac{J'}{4}\sum_i^{N/3}\left(\sigma_i^x\sigma_{i+1}^x + \sigma_i^y\sigma_{i+1}^y + \Delta'\sigma_i^z\sigma_{i+1}^z\right), \quad (5)$$

where the iterative relationship is

$$J' = J\left(\frac{2q}{2+q^2}\right)^2, \quad \Delta' = \Delta\frac{q^2}{4}. \quad (6)$$

The most important information given in the QRG method are its fixed points. By solving equation $\Delta' = \Delta$, we obtain the trivial fixed point $\Delta = 0$ and also the nontrivial fixed point $\Delta = 1$. It is worth noticing that, as was stated previously, XXZ model is critical for all $0 \leqslant \Delta \leqslant 1$ while QRG method only indicates the single points. Indeed, if appropriate boundary terms are implemented in the QRG method, then it predicts correctly a line of critical models in the range $0 \leqslant \Delta \leqslant 1$ [35].

In order to calculate quantum discord and other correlation quantities, we consider one of the degenerate ground states. Correspondingly, the density matrix is defined as

$$\rho_{123} = |\phi_0\rangle\langle\phi_0|, \quad (7)$$

with $|\phi_0\rangle$ referring to Eq. (2) (choosing $|\phi_0'\rangle$ will yield the same results). Since we are focusing on pairwise correlation functions, without loss of generality, we trace over site 2 to obtain the reduced density matrix between sites 1 and 3,

$$\rho_{13} = \frac{1}{2+q^2}\begin{pmatrix} q^2 & 0 & 0 & 0 \\ 0 & 1 & 1 & 0 \\ 0 & 1 & 1 & 0 \\ 0 & 0 & 0 & 0 \end{pmatrix}. \quad (8)$$

It is straightforward to compute the concurrence [36] of ρ_{13},

$$C_{13} = \frac{2}{2+q^2}. \quad (9)$$

It is shown that the concurrence between two blocks exhibits an explicit signature of the quantum phase transitions at $\Delta = 1$. Meanwhile, we notice that some other entanglement measures in the literature, such as von Neumann entropy or the averaged bipartite entanglement, are shown to be good indicators of the quantum phase transition. However, to our best knowledge, there is no study of analyzing other correlation witnesses beyond entanglement in QRG framework. In the below section, we will analytically derive these quantities in detail to see whether they can be proved helpful in predicting critical phenomenon.

A. Quantum discord and measurement-induced disturbance

Quantum discord is introduced in Ref. [3] aiming to characterize all the nonclassical correlations present in a bipartite state. It originates from the inequivalence of two expressions of mutual information in the quantum realm. Consider a composite bipartite system ρ^{AB}, where the quantum mutual information is defined as

$$\mathcal{I}(\rho^{AB}) := S(\rho^A) + S(\rho^B) - S(\rho^{AB}), \quad (10)$$

where $S(\rho) = -\text{Tr}(\rho\log_2\rho)$ is the von Neumann entropy and $\rho^{A(B)} = \text{Tr}_{B(A)}(\rho^{AB})$ denote the reduced density operator of

subsystem $A(B)$. On the other hand, if a complete set of von Neumann measurements $\{\Pi_k^A\}$ (or, more generally, POVMs) performed on subsystem A, an alternative version of quantum mutual information conditioned on this measurement yields

$$\mathcal{I}\left(\rho\middle|\{\Pi_k^A\}\right) := S(\rho^B) - S\left(\rho\middle|\{\Pi_k^A\}\right), \tag{11}$$

$$= S(\rho^B) - \sum_k p_k S\left(\rho_k^B\right), \tag{12}$$

with $p_k = \mathrm{Tr}(\Pi_k^A \rho^{AB})$ and $\rho_k^B = \mathrm{Tr}_A(\Pi_k^A \rho^{AB})/p_k$. To eliminate the dependence on specific measurement, one takes the optimization procedure to obtain

$$\mathcal{J}(\rho) := \max_{\{\Pi_k^A\}} \mathcal{I}\left(\rho\middle|\{\Pi_k^A\}\right), \tag{13}$$

which has been suggested by Henderson and Vedral [4] as a measure to quantify the purely classical part of correlations. The discrepancy between the original quantum mutual information $\mathcal{I}$ and the measurement-induced quantum mutual information $\mathcal{J}$ is defined as the so-called quantum discord

$$\mathcal{D}_A(\rho) := \mathcal{I}(\rho) - \mathcal{J}(\rho), \tag{14}$$

$$= S(\rho^A) - S(\rho^{AB}) + \min_{\{\Pi_k^A\}} \sum_k p_k S\left(\rho_k^B\right). \tag{15}$$

Now we are going to deal with the situation that we come across. The density matrix defined in Eq. (8) is a two-qubit X-shaped state. A general X state look like this:

$$\rho^\chi = \begin{pmatrix} \rho_{11} & 0 & 0 & \rho_{14} \\ 0 & \rho_{22} & \rho_{23} & 0 \\ 0 & \rho_{23}^* & \rho_{33} & 0 \\ \rho_{14}^* & 0 & 0 & \rho_{44} \end{pmatrix}, \tag{16}$$

which has seven real parameters. However, up to local unitary equivalence, we can assume ρ_{14} and ρ_{23} are also real and, in fact, there are only five independent parameters (note that QD is invariant under local unitary transformations). Alternatively, if we represent the X state in Bloch decomposition, then the five characterizing parameters can be expressed as

$$\begin{aligned} x &= \mathrm{Tr}\left(\sigma_z^A \rho^\chi\right) = \rho_{11} + \rho_{22} - \rho_{33} - \rho_{44}, \\ y &= \mathrm{Tr}\left(\sigma_z^B \rho^\chi\right) = \rho_{11} - \rho_{22} + \rho_{33} - \rho_{44}, \\ t_1 &= \mathrm{Tr}\left(\sigma_x^A \sigma_x^B \rho^\chi\right) = 2\rho_{14} + 2\rho_{23}, \\ t_2 &= \mathrm{Tr}\left(\sigma_y^A \sigma_y^B \rho^\chi\right) = -2\rho_{14} + 2\rho_{23}, \\ t_3 &= \mathrm{Tr}\left(\sigma_z^A \sigma_z^B \rho^\chi\right) = \rho_{11} - \rho_{22} - \rho_{33} + \rho_{44}. \end{aligned} \tag{17}$$

Except for some numerical evaluations for a restricted subset of two-qubit X states [37,38], Ref. [39] presented an algorithm to calculate QD for general two-qubit X states, where the optimal measurement is in a universal finite set $\{\sigma_x, \sigma_y, \sigma_z\}$ (see also Refs. [40,41]). Nonetheless, a counterexample is given by Ref. [42] to disprove the algorithm and this fact elucidates the state dependence in the optimization for general X states. Furthermore, recent progress toward this problem has been made by Ref. [40,41], which identifies a large class of X states whose QD can be derived analytically from the measurement strategy described above.

Keeping these technical preparations in mind, let us turn to density matrix (8), the spectrum of which is $\lambda(\rho_{13}) = \{0, 0, \frac{2}{2+q^2}, \frac{q^2}{2+q^2}\}$. First, we note that $\rho_{22} = \rho_{33}$ and then

$$S(\rho^A) = S(\rho^B) = \frac{1}{2+q^2} \begin{pmatrix} 1+q^2 & 0 \\ 0 & 1 \end{pmatrix}, \tag{18}$$

which means $\mathcal{D}_A(\rho) = \mathcal{D}_B(\rho)$ [4] (here A and B denotes sites 1 and 3, respectively). According to the theorem in Ref. [40], it is easy to check that the optimal observable for state (8) is not σ_z but σ_x. For a reason that will be clear later, we also give discord measured by σ_z (for brevity, we put the general formulas in the Appendix), which is actually equal to the concurrence

$$\mathcal{D}_A^{\sigma_z} = \frac{2}{2+q^2}. \tag{19}$$

When the optimal measurement $\{\frac{1}{2}(I \pm \sigma_x^A)\}$ is performed on A, we directly acquire the QD of state (8),

$$\begin{aligned} \mathcal{D}_A^{\sigma_x} = &-\frac{1+q^2}{2+q^2} \log_2 \left(\frac{1+q^2}{2+q^2}\right) - \frac{1}{2+q^2} \log_2 \left(\frac{1}{2+q^2}\right) \\ &+ \frac{2}{2+q^2} \log_2 \left(\frac{2}{2+q^2}\right) + \frac{q^2}{2+q^2} \log_2 \left(\frac{q^2}{2+q^2}\right) \\ &+ f\left[\frac{4+q^4}{(2+q^2)^2}\right], \end{aligned} \tag{20}$$

where $f(z) := -\frac{1+\sqrt{z}}{2} \log_2 \frac{1+\sqrt{z}}{2} - \frac{1-\sqrt{z}}{2} \log_2 \frac{1-\sqrt{z}}{2}$. Numerical evaluation shows $\mathcal{D}_A = \mathcal{D}_A^{\sigma_x}$ is strictly less than $\mathcal{D}_A^{\sigma_z}$, as we expect.

Based on the definition introduced by Luo [7], measurement-induced disturbance (MID) is defined as the difference of quantum mutual information before and after measurement

$$\mathrm{MID}(\rho_{AB}) = I(\rho_{AB}) - I(\Pi(\rho_{AB})). \tag{21}$$

The measurement $\Pi = \{\Pi_i^A \otimes \Pi_j^B\}$ is induced by the spectral decompositions of the reduced states, $\rho^A = \Sigma_i p_i \rho_i^A$ and $\rho^B = \Sigma_i p_i \rho_i^B$, which leaves the marginal information invariant. By taking $\Pi_i^A = |i\rangle\langle i|$ and $\Pi_j^B = |j\rangle\langle j|$ (which is unique in our case), we have $\Pi(\rho_{AB}) = \frac{1}{2+q^2}\mathrm{diag}\{q^2, 1, 1, 0\}$ and, consequently,

$$\mathrm{MID} = S(\Pi(\rho_{AB})) - S(\rho_{AB}) = \frac{2}{2+q^2}. \tag{22}$$

So MID of state (8) coincides with $\mathcal{D}_A^{\sigma_z}$ and the concurrence. However, this is not a coincidence. In the Appendix we will prove that MID is exactly equal to the QD measured by σ_z for general X-structured states.

In Fig. 1, we illustrate the evolution of QD versus Δ for different QRG steps. Notice that the iterative relationship we adopt here and later in the calculation is Eqs. (4) and (6). The plots of QD cross each other at the critical point $\Delta = 1$. In comparison with the concurrence demonstrated in Ref. [23], QD also develops two saturated values, which are associated with the two different phases, the spin-liquid and Néel phases. Note that after enough iteration steps for $0 \leqslant \Delta < 1$, $D_A \approx 0.412154 < C = 0.5$, while for $\Delta > 1$, $D_A \to 0$. In addition, since MID is exactly equal to the concurrence, the MID can obviously exhibit a QPT at $\Delta = 1$.

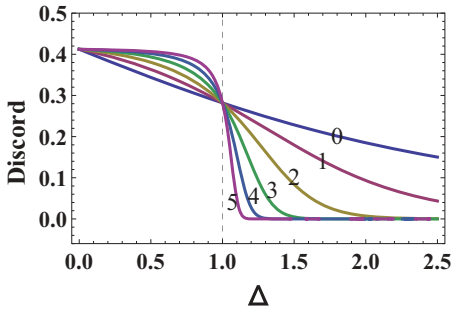

FIG. 1. (Color online) The evolution of the quantum discord versus Δ in terms of QRG iteration steps in the XXZ model.

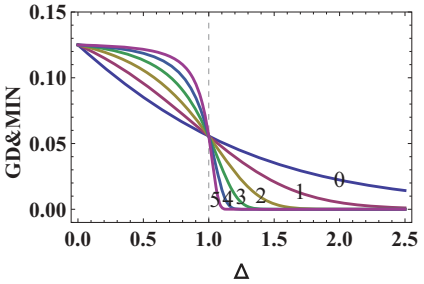

FIG. 2. (Color online) The evolution of the geometric discord and measurement-induced nonlocality versus Δ in terms of QRG iteration steps in the XXZ model.

B. Geometric discord and measurement-induced nonlocality

In this subsection, we calculate GD and MIN. Recently, Dakić *et al*. introduced the following geometric measure of quantum discord based on the Hilbert-Schmidt norm [5]

$$\mathcal{D}_A^G(\rho) := \min_{\chi\in\Omega} \|\rho-\chi\|^2, \tag{23}$$

where Ω denotes the set of zero-discord states and $\|\rho-\chi\|^2 = \mathrm{Tr}(\rho-\chi)^2$ is the square of the Hilbert-Schmidt norm. For the two-qubit case, a closed form of the expression for geometric discord can be achieved,

$$\mathcal{D}_A^G(\rho) = \tfrac{1}{4}(\|\vec{x}\|^2 + \|T\|^2 - \lambda_{\max}), \tag{24}$$

where $x_i = \mathrm{Tr}(\sigma_i^A\rho)$ are components of the local Bloch vector for subsystem A, $T_{ij} = \mathrm{Tr}(\sigma_i^A\sigma_j^B\rho)$ are components of the correlation matrix, and $\vec{x} := (x_1,x_2,x_3)^t$, $T := (T_{ij})$, $\lambda_{\max}$ is the largest eigenvalue of the matrix $K = \vec{x}\vec{x}^t + TT^t$ (here the superscript t denotes transpose). It is worth emphasizing that Luo and Fu presented an equivalent but simplified version of the geometric discord [6]

$$\mathcal{D}_A^G(\rho) = \min_{\Pi^A} ||\rho-\Pi^A(\rho)||^2, \tag{25}$$

where the minimum is over all von Neumann measurements $\Pi^A = \{\Pi_k^A\}$ on subsystem A. Intuitively, in some sense corresponding to GD, another measure quantifying the nonlocal effect caused by locally invariant measurements was introduced Luo and Fu [8]

$$\mathrm{MIN}_A(\rho) = \max_{\Pi^A} ||\rho-\Pi^A(\rho)||^2, \tag{26}$$

with an extra constraint that von Neumann measurements $\Pi^A = \{\Pi_k^A\}$ do not disturb ρ^A locally, which means $\rho^A = \sum_k \Pi_k^A\rho^A\Pi_k^A$.

For the X state and its characterizing parameters defined in Eqs. (17), we have $\vec{x} = (0,0,x)^t$ and $T = \mathrm{diag}\{t_1,t_2,t_3\}$ and GD of the X state reads

$$\mathcal{D}_A^G(\rho^\chi) = \tfrac{1}{4}\left(t_1^2+t_2^2+t_3^2+x^2-\max\left\{t_1^2,t_2^2,t_3^2+x^2\right\}\right), \tag{27}$$

In addition, using theorem 3 in Ref. [8], MIN can be obtained for two-qubit X states

$$\mathrm{MIN}_A(\rho^\chi) = \begin{cases} \frac{1}{4}(t_1^2+t_2^2), & \text{if} \quad x\neq 0 \\ \frac{1}{4}(t_1^2+t_2^2+t_3^2-\lambda_{\min}), & \text{if} \quad x=0 \end{cases}, \tag{28}$$

with $\lambda_{\min} = \min\{t_1^2,t_2^2,t_3^2\}$. Applying these formulas to the state (8), we obtain

$$\mathcal{D}_A^G = \mathrm{MIN}_A = \frac{1}{4}(t_1^2+t_2^2) = \frac{2}{(2+q^2)^2} = \frac{1}{2}C^2, \tag{29}$$

by noting that $t_3^2+x^3 = (\frac{q^2-2}{2+q^2})^2 + (\frac{q^2}{2+q^2})^2 \geqslant (\frac{2}{2+q^2})^2 = t_1^2 = t_2^2$ and $x\neq 0$ since $|q|\geqslant\sqrt{2}$ for $\Delta\geqslant 0$. The variation of GD and MIN versus Δ has been plotted in Fig. 2. It is no surprise that they can indicate the precise location of the critical point $\Delta = 1$ since $\mathcal{D}_A^G = \mathrm{MIN}_A = \frac{1}{2}C^2$.

C. Bell violation

Quantum nonlocality, as revealed by the violation of Bell-type inequalities, refers to many-system measurement correlations that cannot be simulated by any local hidden variable theory. In particular, for two-qubit pure states, the presence of entanglement guarantees violation of a Bell inequality (Gisin's theorem) [43]. However, for mixed stares the situation becomes more complicated [44]. Here we restrict ourselves to the Clauser-Horne-Shimony-Holt (CHSH) inequality. The Bell operator corresponding to CHSH inequality can be formulated in the following form:

$$\mathcal{B}_{\mathrm{CHSH}} = \boldsymbol{a}\cdot\boldsymbol{\sigma}\otimes(\boldsymbol{b}+\boldsymbol{b}')\cdot\boldsymbol{\sigma} + \boldsymbol{a}'\cdot\boldsymbol{\sigma}\otimes(\boldsymbol{b}-\boldsymbol{b}')\cdot\boldsymbol{\sigma}, \tag{30}$$

where $\boldsymbol{a},\boldsymbol{a}',\boldsymbol{b},\boldsymbol{b}'$ are the unit vectors in $\mathbb{R}^3$ and $\boldsymbol{\sigma} = (\sigma_x,\sigma_y,\sigma_z)$. Thee well-known CHSH inequality then is expressed as

$$B = |\langle\mathcal{B}_{\mathrm{CHSH}}\rangle_\rho| = |\mathrm{Tr}(\rho\mathcal{B}_{\mathrm{CHSH}})| \leqslant 2. \tag{31}$$

According to the Horodecki criterion [45], the maximum violation of CHSH inequality is given by

$$\begin{aligned} B_{\mathrm{CHSH}}^{\max} &= \max_{\boldsymbol{a},\boldsymbol{a}',\boldsymbol{b},\boldsymbol{b}'} \mathrm{Tr}(\rho\mathcal{B}_{\mathrm{CHSH}}), \\ &= 2\sqrt{\max_{i<j}(u_i+u_j)}, \end{aligned} \tag{32}$$

where u_i, $i = 1,2,3$ are the eigenvalues of $U = T^tT$.

As for X states, the matrix T is diagonal and $T^tT = \mathrm{diag}\{t_1^2,t_2^2,t_3^2\}$. Therefore, the maximal violation of the CHSH inequality for X states can be simplified to

$$B_{\mathrm{CHSH}}^{\max}(\rho^\chi) = 2\sqrt{\sum_{i=1}^3 t_i^2 - \lambda_{\min}}, \tag{33}$$

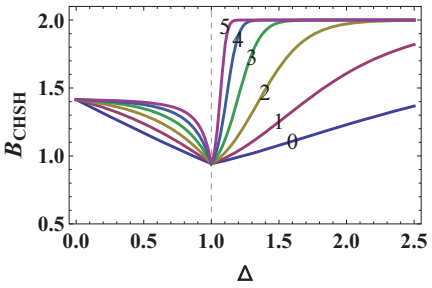

FIG. 3. (Color online) The evolution of the violation of CHSH inequality versus Δ in terms of QRG iteration steps in the XXZ model.

with $\lambda_{\min} = \min\{t_1^2, t_2^2, t_3^2\}$. Thus, the (maximal) Bell violation of state (8) is obtained,

$$B_{\max} = 2\sqrt{\max\left\{\frac{8}{(2+q^2)^2}, \frac{(q^2-2)^2+4}{(2+q^2)^2}\right\}}. \quad (34)$$

The value of maximum Bell violation under QRG iterations is displayed in Fig. 3. Interestingly, we can observe that the block-block correlations never violate the CHSH inequality but still evidently exhibit a QPT. At the critical point $\Delta = 1$, the (maximum) Bell violation is a fixed nonzero constant $B_c = 2\sqrt{2}/3 \approx 0.942809$, irrespective of the iterative steps. What is more, beyond the critical point, Bell violation also develops two saturated values: one is $B = \sqrt{2}$ for $0 \leqslant \Delta < 1$ and one is $B = 2$ for $\Delta > 1$, which is in sharp contrast to the behavior of concurrence.

III. CORRELATION ANALYSIS IN THE ANISOTROPIC XY MODEL

In this section we embark on studying the relationship between the QPT and quantum correlation witnesses in the spin-1/2 XY model with the QRG method. The Hamiltonian of the XY model on a periodic chain with N sites reads

$$H(J,\gamma) = \frac{J}{4}\sum_i^N \left[(1+\gamma)\sigma_i^x\sigma_{i+1}^x + (1-\gamma)\sigma_i^y\sigma_{i+1}^y\right], \quad (35)$$

where J is the exchange coupling constant and γ is the anisotropy parameter. The XY model reduces to the XX model for $\gamma = 0$ or the Ising model for $\gamma = 1$. In the parameter range $0 < \gamma \leqslant 1$, it falls into the Ising universality class. To implement the QRG method, we still choose three sites as a block. In Ref. [26], Ma *et al.* obtained two doubly degenerate eigenvalues of the block Hamiltonian as below

$$|\Phi_0\rangle = \frac{1}{2\sqrt{1+\gamma^2}}(-\sqrt{1+\gamma^2}|\uparrow\uparrow\downarrow\rangle + \sqrt{2}|\uparrow\downarrow\uparrow\rangle - \sqrt{1+\gamma^2}|\downarrow\uparrow\uparrow\rangle + \sqrt{2}\gamma|\downarrow\downarrow\downarrow\rangle), \quad (36)$$

$$|\Phi_0'\rangle = \frac{1}{2\sqrt{1+\gamma^2}}(-\sqrt{2}\gamma|\uparrow\uparrow\uparrow\rangle + \sqrt{1+\gamma^2}|\downarrow\uparrow\uparrow\rangle - \sqrt{2}|\downarrow\uparrow\downarrow\rangle + \sqrt{1+\gamma^2}|\downarrow\downarrow\uparrow\rangle). \quad (37)$$

After projection onto the renormalized subspace, the effective Hamiltonian can be written as

$$H^{\rm eff} = \frac{J'}{4}\sum_i^N \left[(1+\gamma')\sigma_i^x\sigma_{i+1}^x + (1-\gamma')\sigma_i^y\sigma_{i+1}^y\right], \quad (38)$$

with the iterative relationship

$$J' = J\frac{3\gamma^2+1}{2(1+\gamma^2)}, \quad \gamma' = \frac{\gamma^3+3\gamma}{3\gamma^2+1}. \quad (39)$$

Naturally, we are most concerned with the CP information. The stable and unstable fixed points can be gotten by solving $\gamma' = \gamma$. The stable fixed points locate at $\gamma = \pm 1$, and the unstable fixed point is $\gamma = 0$, which separates the spin-fluid phase ($\gamma = 0$) from the the Néel phase ($0 < |\gamma| \leqslant 1$).

Similarly, we consider one of the degeneracy ground states to construct the pure-state density matrix,

$$\varrho_{123} = |\Phi_0\rangle\langle\Phi_0|. \quad (40)$$

The result of choosing $|\Phi_0'\rangle$ will be the same. By tracing out site 2, we arrive at the reduced density matrix

$$\varrho_{13} = \frac{1}{4(\gamma^2+1)}\begin{pmatrix} 2 & 0 & 0 & 2\gamma \\ 0 & \gamma^2+1 & \gamma^2+1 & 0 \\ 0 & \gamma^2+1 & \gamma^2+1 & 0 \\ 2\gamma & 0 & 0 & 2\gamma^2 \end{pmatrix}. \quad (41)$$

The concurrence between the sites 1 and 3 is given as

$$C_{13} = \frac{1}{2} - \frac{|\gamma|}{1+\gamma^2}. \quad (42)$$

A. Quantum discord and measurement-induced disturbance

Before calculating QD and other correlation quantities, we regard all these measures as a function of g, where

$$g = \frac{1+\gamma}{1-\gamma}. \quad (43)$$

The reason is twofold: bringing in such a variable is not only convenient for us to compare the results with that of Ref. [26] but also useful in the derivation process. According to Refs. [40,41], it can be verified that σ_z is not the optimal observable and the choose of optimal observable depends on the value of γ or, more accurately, the sign of γ: The optimal observable to measure is σ_x if $\gamma \geqslant 0$ (which is equivalent to $t_1 \geqslant t_2$ or $|g| \geqslant 1$) and σ_y if $\gamma < 0$ ($|g| < 1$). In spite of this fact, we still provide the discord measured by σ_z here

$$\mathcal{D}^{\sigma_z} = -\frac{1}{2(\gamma^2+1)}\log_2\frac{1}{2(\gamma^2+1)} - \frac{\gamma^2}{2(\gamma^2+1)}\log_2\frac{\gamma^2}{2(\gamma^2+1)}. \quad (44)$$

We again remark that $\varrho_{22} = \varrho_{33}$ for the density matrix (41) and, thus,

$$S(\rho^A) = S(\rho^B) = \frac{1}{4(\gamma^2+1)}\begin{pmatrix} \gamma^2+3 & 0 \\ 0 & 3\gamma^2+1 \end{pmatrix}. \quad (45)$$

So we do not need to specify on which subsystem the measurement is performed. The spectrum of (41) is

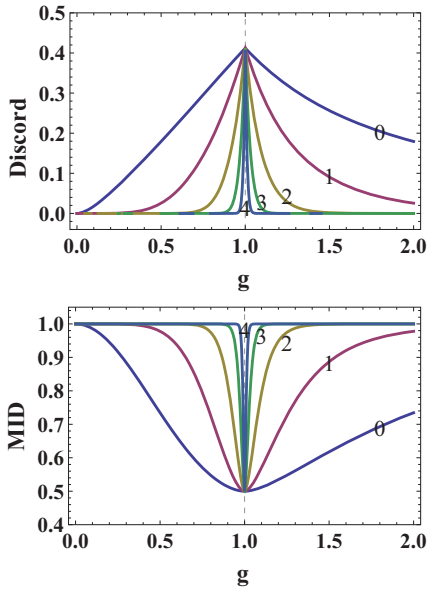

FIG. 4. (Color online) The evolution of quantum discord and measurement-induced disturbance versus Δ in terms of QRG iteration steps in the XY model.

$\lambda(\varrho) = \{1/2,1/2,0,0\}$, irrespective of the value of γ. After some lengthy but standard algebra, one finally gets

$$\begin{aligned}\mathcal{D} &= S(\varrho^A) - S(\varrho^{AB}) + f\left(y^2 + \max\left\{t_{1,2}^2\right\}\right) \\ &= -\frac{\gamma^2+3}{4(\gamma^2+1)}\log_2\frac{\gamma^2+3}{4(\gamma^2+1)} - \frac{3\gamma^2+1}{4(\gamma^2+1)}\log_2\frac{3\gamma^2+1}{4(\gamma^2+1)} \\ &\quad -1 + f\left[\frac{(|\gamma|+1)^2}{2(\gamma^2+1)}\right], \end{aligned} \tag{46}$$

with y, t_1, t_2, and function $f(\cdot)$ defined as above.

From the proof in the Appendix, we already know that MID is exactly equal to $\mathcal{D}^{\sigma_z}$. The QD and MID between site 1 and 3 have been plotted in Fig. 4 [recall that for this model the iterative relationship is just Eq. (39)]. The dynamic behavior of QD in each iteration step is analogous to that of the concurrence but not totally the same. At the critical point $g = 1$, QD reaches a nonzero constant $\mathcal{D} \approx 0.412154$, which once again indicates that the spin-fluid phase contains quantum correlations as already shown in the XXZ model. In contrast to QD, MID also shows the nonanalytic property; however, for $0 \leqslant g < 1$ and $g > 1$ MID does not fall to zero but gets to another nonzero constant MID $= 1$.

B. Geometric discord, measurement-induced nonlocality, and Bell violation

In Sec. II we have obtained the analytic formulas for GD, MIN, and Bell violation. Employing Eqs. (27), (28), and (33), the GD, MIN and Bell violation for state (41) are listed as follows (in the derivation note that $\gamma \geqslant 0$ and $\gamma < 0$ correspond to $|g| \geqslant 1$ and $|g| < 1$, respectively):

$$\mathcal{D}^G = \frac{1}{4}\left(\frac{1}{2} - \frac{|\gamma|}{1+\gamma^2}\right) = \frac{1}{4}C, \tag{47}$$

$$\mathrm{MIN} = \frac{\gamma^4 + 6\gamma^2 + 1}{8(\gamma^2+1)^2}, \tag{48}$$

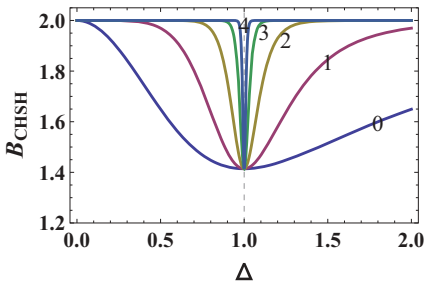

FIG. 5. (Color online) The evolution of the violation of CHSH inequality versus Δ in terms of QRG iteration steps in the XY model.

$$B_{\max} = \frac{\sqrt{2\gamma^4 + 12\gamma^2 + 2}}{\gamma^2+1} = 4\sqrt{\mathrm{MIN}}. \tag{49}$$

Here the Bell violation versus g changing for different iterations is depicted in Fig. 5. It is clearly seen that in the XY model the block-block correlation is still not strong enough to violate the CHSH inequality although Bell violation displays the nonanalytic behavior at $g = 1$ ($\gamma = 0$).

IV. NONANALYTIC AND SCALING BEHAVIOR

So far, we have employed the QRG method to investigate the *block-block correlations* of one-dimensional XXZ and XY spin models. As we have described in the QRG approach, the size of a large system ($N = 3^{n+1}$) can be effectively rescaled to three sites with the renormalized couplings of the nth RG iteration. Therefore, the quantum correlations between the two renormalized sites represent the correlations between two parts of the system, each effectively containing $N/3$ sites. In this sense, we can refer to these quantities considered in this work as block-block correlations. It has been demonstrated that the first derivative of all these correlation measures shows a nonanalytic behavior in the vicinity of the critical point. Furthermore, the scaling property of entanglement has also been observed in Refs. [23,26], which is related to the divergence of the correlation length as the critical point is approached.

Aiming to compare with the previous results concerning entanglement, we explicitly show the nonanalytic phenomenon and scaling behavior of other correlation witnesses. Here, we

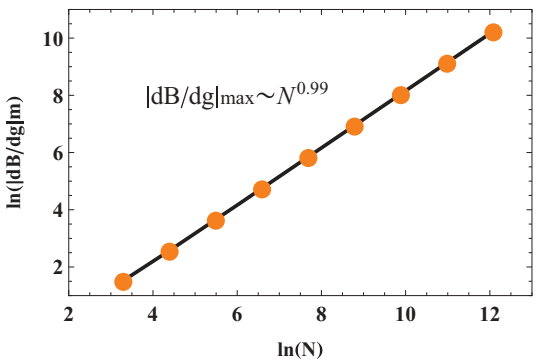

FIG. 6. (Color online) The logarithm of the absolute value of minimum, $\ln(|dB/dg|_{\mathrm{m}})$, versus the logarithm of chain size, $\ln(N)$, which is linear and displays a scaling behavior (B is the Bell violation in the XY model).

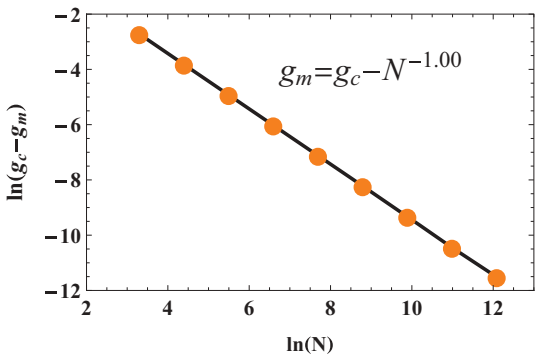

FIG. 7. (Color online) The scaling behavior of $g_{\max}$ in terms of system size N, where $g_{\max}$ is the position of the minimum derivative of Bell violation in the XY model.

focus on the dynamic property of nonlocality, that is, the maximal violation of the Bell-CHSH inequality, since our results display that quantum discord behaves more similarly to entanglement (see Figs. 1 and 4). First, we have analyzed the scaling behavior of $y = |dB/dg|_{g_m}$ versus the size of the system N in the XY model where g_m is the position of the minimum of dB/dg. We have plotted $\ln(y)$ versus $\ln(N)$ in Fig. 6, which shows a linear behavior. Numerical calculation tells us that the exponent for this behavior is $|dB/dg|_{g_m} \sim N^{0.99}$. As a companion, our analysis also reveals that the position of the minimum g_m of dB/dg gradually tends to the critical point $g_c = 1$, as shown in Fig. 7 (the numerical relation is $g_m = g_c - N^{-1.00}$). These results convince us that the Bell violation truly signifies the criticality of the spin system.

V. DISCUSSION AND CONCLUSION

In this paper, we have investigated the performance of various correlation measures in the quantum phase transition, exploiting the quantum renormalization-group method. In most of the previous literature, only entanglement (concurrence) has been utilized as an information-theoretic tool to evaluate the critical properties of the spin systems. However, it is now well known that entanglement cannot account for all aspects of quantum correlations, which, in turn, motivates us to clarify whether other correlations (including Bell-CHSH violation) are useful in such a circumstance. Indeed, there are several points that deserve our attention: (i) The quantum discord and other discordlike measures turn out to be as good as entanglement to detect the quantum phase transition in the anisotropic XXZ and XY models. Nevertheless, it is apparent that the dynamic processes of these quantities are not totally similar with entanglement and even when concurrence vanishes there still exists some kind of quantum correlation which is not captured by entanglement. (ii) Interestingly, our result shows that CHSH inequality can never be violated in the entire iteration procedure, which indicates the block-block entanglement cannot be revealed by the CHSH inequality. Moreover, the nonanalytic and scaling behaviors of Bell violation have been justified by numerical calculations.

On the other hand, the two cases handled in this work can be regard as perfect examples to apply the QD algorithm raised in Refs. [40,41], where the optimal measurements to achieve QD can be exactly determined. In addition, we are convinced that the whole analysis in this paper can be extended to many other spin models, since the reduced density matrices are usually highly symmetric and can be cast into X-shaped states [24,25,27,31,32]. Very recently, it has been reported that Bell inequality is able to signal QPT and it can never be violated in the corresponding spin models [46,47]. In these works, the nearest-neighboring spin-spin correlation functions are invoked to compute the Bell violation, which is usually complex and lengthy. However, we resort to the QRG framework and also illustrate that no violation can be discovered in each iteration step, which implies some intrinsic feature of long-scale corrections. The connection between these observations will be attractive and may need further investigation. Finally, we would like to mention that it might be interesting to apply the same approach to high-dimensional systems, where a straightforward numerical analysis could be performed for some measures of quantum correlations.

ACKNOWLEDGMENTS

This work was supported by the National Basic Research Program of China (Grants No. 2011CBA00200 and No. 2011CB921200), National Natural Science Foundation of China (Grant NO. 60921091), and China Postdoctoral Science Foundation (Grant No. 20100480695).

APPENDIX A: ANALYTIC PROOF OF MID = $\mathcal{D}^{\sigma_z}$ FOR GENERAL X STATES

Here we show that measurement-induced disturbance is exactly equal to the quantum discord measured by σ_z for general X-structured states. The expressions of QD and MID are formulated as follows:

$$\mathcal{D}_A(\rho) = S(\rho^A) - S(\rho) + \min_{\{\Pi_k^A\}} \sum_k p_k S\left(\rho_k^B\right), \tag{A1}$$

$$\mathrm{MID}(\rho) = I(\rho) - I(\Pi(\rho)) = S(\Pi(\rho)) - S(\rho). \tag{A2}$$

Note that the two-sided measurements $\Pi = \{\Pi_i^A \otimes \Pi_j^B\}$ employing in MID depend on the spectral decompositions of the reduced states. Since we only consider the discord measured by σ_z, that is, $\{\frac{1}{2}(I \pm \sigma_z)\} = \{|0\rangle\langle 0|, |1\rangle\langle 1|\}$, the conditional states for general X states (16) can be obtained,

$$\begin{aligned} \rho_0^B &= \frac{1}{\rho_{11}+\rho_{22}} \begin{pmatrix} \rho_{11} & 0 \\ 0 & \rho_{22} \end{pmatrix}, \\ \rho_1^B &= \frac{1}{\rho_{33}+\rho_{44}} \begin{pmatrix} \rho_{33} & 0 \\ 0 & \rho_{44} \end{pmatrix}, \end{aligned} \tag{A3}$$

with $p_0 = \rho_{11} + \rho_{22}$ and $p_1 = \rho_{33} + \rho_{44}$. The reduced states are all diagonal states,

$$\begin{aligned} \rho^A &= \begin{pmatrix} \rho_{11}+\rho_{22} & 0 \\ 0 & \rho_{33}+\rho_{44} \end{pmatrix}, \\ \rho^B &= \begin{pmatrix} \rho_{11}+\rho_{33} & 0 \\ 0 & \rho_{22}+\rho_{44} \end{pmatrix}. \end{aligned} \tag{A4}$$

Therefore, we can take $\Pi_i^A = |i\rangle\langle i|$, $\Pi_j^B = |j\rangle\langle j|$ $(i, j = 0, 1)$. To prove $\mathrm{MID} = \mathcal{D}^{\sigma_z}$, all we need is to verify

$S(\rho^A) + \sum_k p_k S(\rho_k^B) = S(\Pi(\rho))$. In fact, it is easy to find

$$S(\rho^A) + \sum_k p_k S\left(\rho_k^B\right) = -\sum_{ii} \rho_{ii} \log_2(\rho_{ii}) = S(\Pi(\rho)) \tag{A5}$$

with $ii = 11,22,33,44$. Moreover, when the measurement σ_z is performed on subsystem B, the situation is the same. To sum up, we arrive at the relationship $\mathcal{D}_A^{\sigma_z} = \mathcal{D}_B^{\sigma_z} =$ MID for X states.

APPENDIX B: ANALYTIC FORMULA OF $\mathcal{D}^{\sigma_x}(\mathcal{D}^{\sigma_y})$ FOR GENERAL X STATES

By definition, we need to evaluate the conditional state ρ_k^B and the corresponding probability p_k, since $S(\rho^A)$ and $S(\rho^{AB})$ are easy to compute. Let $\{\Pi_k^A = \frac{1}{2}(I \pm \sigma_x)\}$ $(k = \pm)$ be the local measurement for subsystem A, then

$$\begin{aligned}\rho_\pm^B &= \frac{1}{p_\pm} \mathrm{Tr}_A(\Pi_\pm^A \otimes I^B \rho \Pi_\pm^A \otimes I^B), \\ &= \begin{bmatrix} \rho_{11} + \rho_{33} & \pm(\rho_{14} + \rho_{23}) \\ \pm(\rho_{14} + \rho_{23}) & \rho_{22} + \rho_{44} \end{bmatrix}, \\ &= \frac{1}{2} \begin{pmatrix} 1 + y & \pm t_1 \\ \pm t_1 & 1 - y \end{pmatrix}, \end{aligned} \tag{B1}$$

with $p_k = \mathrm{Tr}(\Pi_\pm^A \otimes I^B \rho \Pi_\pm^A \otimes I^B) = \frac{1}{2}$, $k = \pm$, and y, t_1 defined in Eqs. (17). In addition, $\rho_\pm^B$ have exactly the same spectrum,

$$\lambda(\rho_k) = \tfrac{1}{2}\left(1 \pm \sqrt{y^2 + t_1^2}\right). \tag{B2}$$

Therefore,

$$\begin{aligned}\sum_k p_k S\left(\rho_k^B\right) &= S(\rho_+^B) = S(\rho_-^B), \\ &= f\left(y^2 + t_1^2\right). \end{aligned} \tag{B3}$$

where $f(z) := -\frac{1+\sqrt{z}}{2} \log_2 \frac{1+\sqrt{z}}{2} - \frac{1-\sqrt{z}}{2} \log_2 \frac{1-\sqrt{z}}{2}$. If we choose $\{\Pi_k^A = \frac{1}{2}(I \pm \sigma_y)\}$ as the local measurement on A, an analogous expression can be achieved,

$$\sum_k p_k S\left(\rho_k^B\right) = f\left(y^2 + t_2^2\right). \tag{B4}$$

According to Ref. [40,41], as long as

$$|\sqrt{\rho_{11}\rho_{44}} - \sqrt{\rho_{22}\rho_{33}}| \leqslant |\rho_{14}| + |\rho_{23}| \tag{B5}$$

holds, the optimal observable is σ_x if $t_1 \geqslant t_2$ and σ_y otherwise. Consequently,

$$\mathcal{D}_A(\rho) = S(\rho^A) - S(\rho^{AB}) + f\left(y^2 + \max\left\{t_{1,2}^2\right\}\right). \tag{B6}$$

Note that $S(\rho^A)$ and $S(\rho^{AB})$ can also be represented by parameters defined in Eqs. (17) (see Eq. (8) in Ref. [41]).

[1] A. Einstein, B. Podolsky, and N. Rosen, Phys. Rev. **47**, 777 (1935).
[2] M. A. Nielsen and I. L. Chuang, *Quantum Computation and Quantum Communication* (Cambridge University Press, Cambridge, 2000).
[3] H. Ollivier and W. H. Zurek, Phys. Rev. Lett. **88**, 017901 (2001).
[4] L. Henderson and V. Vedral, J. Phys. A **34**, 6899 (2001).
[5] B. Dakić, V. Vedral, and C. Brukner, Phys. Rev. Lett. **105**, 190502 (2010)
[6] S. Luo and S. Fu, Phys. Rev. A **82**, 034302 (2010).
[7] S. Luo, Phys. Rev. A **77**, 022301 (2008).
[8] S. Luo and S. Fu, Phys. Rev. Lett. **106**, 120401 (2011).
[9] S. Wu, U. V. Poulsen, and K. Mølmer, Phys. Rev. A **80**, 032319 (2009).
[10] K. Modi, A. Brodutch, H. Cable, T. Paterek, and V. Vedral, arXiv:1112.6238.
[11] S. Sachdev, *Quantum Phase Transitions* (Cambridge University Press, Cambridge, UK, 2000).
[12] A. Osterloh, L. Amico, G. Falci, and R. Fazio, Nature (London) **416**, 608 (2002).
[13] T. J. Osborne and M. A. Nielsen, Phys. Rev. A **66**, 032110 (2002).
[14] G. Vidal, J. I. Latorre, E. Rico, and A. Kitaev, Phys. Rev. Lett. **90**, 227902 (2003).
[15] L.-A. Wu, M. S. Sarandy, and D. A. Lidar, Phys. Rev. Lett. **93**, 250404 (2004).
[16] L. Amico, R. Fazio, A. Osterloh, and V. Vedral, Rev. Mod. Phys. **80**, 517 (2008).
[17] R. Dillenschneider, Phys. Rev. B **78**, 224413 (2008).
[18] M. S. Sarandy, Phys. Rev. A **80**, 022108 (2009).
[19] T. Werlang, C. Trippe, G. A. P. Ribeiro, and G. Rigolin, Phys. Rev. Lett. **105**, 095702 (2010).
[20] K. G. Wilson, Rev. Mod. Phys. **47**, 773 (1975).
[21] P. Pfeuty, R. Jullian, K. L. Penson, in *Real-Space Renormalization*, edited by T. W. Burkhardt and J. M. J. van Leeuwen (Springer, Berlin, 1982), chap. 5.
[22] M. Kargarian, R. Jafari, and A. Langari, Phys. Rev. A **76**, 060304 (2007).
[23] M. Kargarian, R. Jafari, and A. Langari, Phys. Rev. A **77**, 032346 (2008).
[24] R. Jafari, M. Kargarian, A. Langari, and M. Siahatgar, Phys. Rev. B **78**, 214414 (2008).
[25] M. Kargarian, R. Jafari, and A. Langari, Phys. Rev. A **79**, 042319 (2009).
[26] F. W. Ma, S. X. Liu, and X. M. Kong, Phys. Rev. A **83**, 062309 (2011).
[27] F. W. Ma, S. X. Liu, and X. M. Kong, Phys. Rev. A **84**, 042302 (2011).
[28] J. S. Bell, Physics (Long Island City, NY) **1**, 195 (1964).
[29] J. F. Clauser, M. A. Horne, A. Shimony, and R. A. Holt, Phys. Rev. Lett. **23**, 880 (1969).
[30] M. A. Martin-Delgado and G. Sierra, Int. J. Mod. Phys. A **11**, 3145 (1996).
[31] A. Langari, Phys. Rev. B **58**, 14467 (1998); **69**, 100402(R) (2004)
[32] R. Jafari and A. Langari, Phys. Rev. B **76**, 014412 (2007); Physica A **364**, 213 (2006).

[33] S.-J. Gu, H.-Q. Lin, and Y.-Q. Li, Phys. Rev. A **68**, 042330 (2003).
[34] S.-J. Gu, G.-S. Tian, and H.-Q. Lin, Phys. Rev. A **71**, 052322 (2005).
[35] M. A. Martin-Delgado and G. Sierra, Phys. Rev. Lett. **76**, 1146 (1996).
[36] W. K. Wootters, Phys. Rev. Lett. **80**, 2245 (1998)
[37] J. Maziero, T. Werlang, F. F. Fanchini, L. C. Celeri, and R. M. Serra, Phys. Rev. A **81**, 022116 (2010).
[38] F. F. Fanchini, T. Werlang, C. A. Brasil, L. G. E. Arruda, and A. O. Caldeira, Phys. Rev. A **81**, 052107 (2010).
[39] M. Ali, A. R. P. Rau, and G. Alber, Phys. Rev. A **81**, 042105 (2010).
[40] Q. Chen, C. Zhang, S. Yu, X. X. Yi, and C. H. Oh, Phys. Rev. A **84**, 042313 (2011).
[41] S. Yu, C. Zhang, Q. Chen, and C. H. Oh, arXiv:1102.1301.
[42] X.-M. Lu, J. Ma, Z. Xi, and X. Wang, Phys. Rev. A **83**, 012327 (2011).
[43] N. Gisin, Phys. Lett. A **154**, 201 (1991).
[44] R. F. Werner, Phys. Rev. A **40**, 4277 (1989).
[45] R. Horodecki, P. Horodecki, and M. Horodecki, Phys. Lett. A **200**, 340 (1995); R. Horodecki, *ibid.* **210**, 223 (1996).
[46] J. Batle and M. Casas, Phys. Rev. A **82**, 062101 (2010).
[47] L. Justino and Thiago R. de Oliveira, Phys. Rev. A **85**, 052128 (2012).